Global NEST Journal, Vol 22, No 1, pp 119-125

Photocatalytic reduction of $AuCl_4^-$ by $Fe_3O_4/SiO_2/TiO_2$ nanoparticles

Kunarti E.S.*, Roto R., Nuryono N., Santosa S.J. and Fajri M.L.
Chemistry Department, Faculty of Mathematics and Natural Sciences, Universitas Gadjah Mada, Yogyakarta, Indonesia
Received: 05/12/2019, Accepted: 18/02/2020, Available online: 12/03/2020
*to whom all correspondence should be addressed: e-mail: eko_kunarti@ugm.ac.id
https://doi.org/10.30955/gnj.003262

Graphical abstract

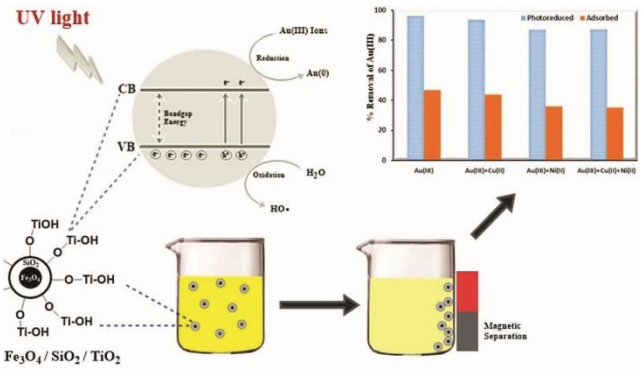

Abstract

Metallurgy and recovery of gold in electronic waste sometimes involve the reduction of tetrachloroaurate ion ($AuCl_4^-$) to elemental gold form. Currently, for the reduction of tetrachloroaurate ion, people use reducing agents such as hydroquinone and sodium borohydride. Photocatalysts of $Fe_3O_4/SiO_2/TiO_2$ nanoparticles were prepared and tested for the reduction of tetrachloroaurate ion under UV light illumination. The magnetite (Fe_3O_4) nanoparticle was first prepared by coprecipitation and sonication, followed by SiO_2 and TiO_2 coatings via the sol-gel process and calcination. The products were confirmed by XRD and TEM. The photocatalytic reduction of tetrachloroaurate ion was performed in a closed reactor equipped with a UV light source. The results indicated that $Fe_3O_4/SiO_2/TiO_2$ nanoparticles were successfully prepared, which retained good magnetic and photocatalytic properties. The photocatalytic reaction is best performed at a pH of 5 under UV irradiation for 2 h, which is capable of reducing 96% of the tetrachloroaurate present in the mixture. The co-presence of Ni^{2+} and Cu^{2+} ions in the solution leads to a decrease in yield due to competitive reduction and adsorption. The photocatalyst is recoverable by the use of a magnetic bar and may find application for gold recovery and metallurgy.

Keywords: Nanoparticle, $Fe_3O_4/SiO_2/TiO_2$, photoreduction, tetrachloroaurate.

1. Introduction

Gold is one of the precious metals, well-known for its beauty, corrosion resistance, malleability, and ease to form alloys. It has been used to prepare coins and jewelry since ancient times. Along with technological advances, gold is now used in the production of electronic devices for its excellent electrical conductivity. The rapid technological progress and consumptive nature of society lead to the shortening of the use of electronic devices, which use gold in many of their components. It speeds up the discharge of electronic devices waste. Among other rare earth metal elements, the valuable component of the electronic device waste is gold.

Roughly, the waste of electronic devices contains 40% of metals, including heavy metals such as copper (20%), tin (4%), nickel (2%), lead (2%), silver (0.02%) and precious metals such as gold (0.1%) (Gramatyka *et al.*, 2007). Therefore, metal recovery of electronics waste is an important way, not only from the management of hazardous waste point of view but also from the recovery process of the precious metals.

The process of gold recovery from electronic equipment waste requires several steps that are dissolution, separation, and purification (Cui and Zhang, 2008). In the purification step, the photocatalytic reduction method is usually applied by utilizing a semiconductor, which is relatively new and potentially useful as an alternative green method. More importantly, it does not produce harmful by-products (Kida *et al.*, 2009; Barakat, 2010).

Titanium dioxide is often used as a photocatalyst because of its low toxicity, superior photocatalytic performance, and good chemical stability. Several studies on the application of titanium dioxide for gold recovery have been reported, such as by Grieken *et al.* (2005) who have reviewed the gold recovery process from electroplating waste in the $[Au(CN)_2]^-$ complex using a titanium dioxide photocatalyst. Wojnicki *et al.* (2013) have conducted a study of gold photoreduction kinetics in the complex form $AuCl_4^-$ using TiO_2. Wahyuni *et al.* (2015) have successfully examined the application of gold recovery by photocatalytic reduction of $AuCl_4^-$ ion by utilizing TiO_2

photocatalyst with the addition of other metal ions such as Ag(I), Cu^{2+}, and Fe^{3+}.

The photocatalytic reaction commonly takes place in the suspension of a photocatalyst having a nanometer size, so that an efficient separation process is required to recover the catalyst from the aqueous medium. Several studies have been conducted regarding suspended TiO_2 separation efforts in heterogeneous photocatalysis processes, e.g., flocculation, sedimentation and microfiltration (Xi and Geissen, 2001; Rottman, 2013). But such methods need additional costs for chemicals, takes a relatively long time, are relatively expensive and need control during the separation process.

Photocatalysts such as glass beads, silica gel, glass fibers in mesh form, and zeolites are coated with titanium to alleviate the problem (Szabo *et al.*, 2013). Although this method can provide solutions to problems related to the difficulty of liquid-solid phase separation, slurry-type reactors are more advantageous than immobilized photocatalyst systems in terms of available surface area and better mass-transfer characteristics. The magnetization of the photocatalyst can facilitate the process of photocatalyst recovery with the help of a magnetic bar. This modification is able to combine the characteristics of the surface to volume ratio and settling process commonly observed by larger particles (Beydoun *et al.*, 2000).

The TiO_2 modification of the catalyst can be done by superimposing on the surface of the magnetic material. Beydoun *et al*. (2000) have reported work on the modification of magnetite by superimposing with titania to give photocatalyst nanocomposite. However, direct contact between the titania and iron oxide could lower photocatalytic activity and cause a photo dissolution event. To avoid this problem, in the later research Beydoun and Amal (2002) modified magnetite by coating with SiO_2 as an insulating layer for direct charge transfer between Fe_3O_4 core and TiO_2 shell. The SiO_2 layer with porous structures enables the surface area to increase and to facilitate better access for target species to reach the active site of the material (Ullah *et al.*, 2015). Several studies on addition of SiO_2 layer to the Fe_3O_4/TiO_2 nanocomposite show a better performance in photooxidation of organic compounds such as sucrose (Beydoun and Amal, 2002), methyl orange (Gad-Allah
et al., 2007), acetaminophen, antipyretin, caffeine, metoprolol, bisphenol A (Álvarez *et al*., 2010), methylene blue (Kunarti *et al.*, 2016) and photoreduction of silver(I) ions (Kunarti *et al*., 2017). We have been working on the photocatalytic reduction of metallic ions (Kunarti *et al.*, 2017; Fajri, 2017). In this contribution, photocatalytic reduction of tetrachloroaurate ion by $Fe_3O_4/SiO_2/TiO_2$ nanoparticles is reported. This work is novel since the photoreduction of tetrachloroaurate ion using this type of photocatalyst has not been reported elsewhere. In addition, the photoreduction of tetrachloroaurate is usualy done with TiO_2 photocatalyst. The introduction of magnetic material of magnetite to the TiO_2 photocatalyst allows us to separate and reuse the photocatalyst. Further, the effect of some operating conditions such as pH and time is evaluated. In addition, the co-presence of Cu^{2+} and Ni^{2+} that are commonly found along with $AuCl_4^-$ is also examined. These two metals are also present in the minerals containing gold.

2. Materials and methods

2.1. Chemicals

Iron(II) chloride tetrahydrate ($FeCl_2{\cdot}4H_2O$), iron(III) chloride hexahydrate ($FeCl_3{\cdot}6H_2O$), tetraethyl orthosilicate (TEOS, >99%), trisodium citrate dihydrate ($Na_3C_6H_5O_7{\cdot}2H_2O$), ethanol, ammonia solution (25% v/v), tetrachloroauric acid ($HAuCl_4$) were purchased from Merck. Titanium(IV) tetraisopropoxide (TTIP, >97%) was acquired from Aldrich. Deionized water was used as the main solvent throughout the experiments. The chemicals were used as received without further purification.

2.2. Preparation of $Fe_3O_4/SiO_2/TiO_2$ nanoparticles

Magnetite, Fe_3O_4, and Fe_3O_4/SiO_2 nanoparticles were prepared according to the previous work (Kunarti *et al.*, 2017) with slight modification. They were synthesized through a sol-gel method. Briefly, Fe_3O_4/SiO_2 was dispersed in 30 mL ethanol 98% followed by the addition of 0.20 mL deionized water and 1 mL TTIP. The mixture was ultrasonicated for 3 hours. The produced material was washed with ethanol several times. The solids were dried, and the product obtained was calcined at 500 °C for 3 h. The as prepared $Fe_3O_4/SiO_2/TiO_2$ nanoparticles were characterized and then applied for the recovery of gold through photoreduction of tetrachloroauric ions.

2.2.1. Product characterization and analysis

X-ray diffraction patterns were recorded on Shimadzu XRD 6000, with Cu-Kα radiation. The XRD patterns were used to confirm the crystal structure of the synthesized materials. Transmission electron microscopy (TEM) images were obtained on JEOL JEM-1400 TEM with an acceleration voltage of 120 kV. The magnetic properties were quantified using a cryogen-free physical measurement vibrating sample magnetometer (Oxford VSM 1.2H). The tetrachloroaurate ions in the solution were determined by using atomic absorption spectrometry (AAS) (Perkin Elmer 3110).

2.3. Photocatalytic reduction of tetrachloroauric

The photoreduction of tetrachloroaurate ion was performed in a batch system in a closed vessel equipped with a UV-lamp (40 W, 220 V, wavelength 340-390 nm). A 25 mL $AuCl_4^-$ solution of 50 mg/L, and the catalyst weighed 0.025 g were placed in the glass vessel. The nanoparticles were dispersed by stirring the suspension continuously using magnetic stirrer under UV-irradiation. After the reaction, the solution tetrachloroaurate ions were analyzed by AAS. In this study, the effect of pH and time, and the addition of Cu^{2+}, and Ni^{2+} ions were also studied. The predetermined condition is presented in Table 1.

Table 1. Prescribed experimental condition for the photocatalytic reduction of $[AuCl_4]^-$

Variable	Preset
pH	1, 3, 5, 7, 9
Reaction time (h)	0.5, 1, 2, 3, 4
Mas of photocatalyst (mg)	25
Concentration of $AuCl_4^-$ (mg/L)	50
Concentration of Ni^{2+} (mg/L)	50
Concentration of Cu^{2+} (mg/L)	50

2.3.1. Reduction of $AuCl_4^-$ ions in a mixture with Cu^{2+} or Ni^{2+}

A portion of 0.025 g of $Fe_3O_4/SiO_2/TiO_2$ nanoparticles photocatalyst was incorporated into the mixture of $[AuCl_4]^-$ and Cu^{2+}(or Ni^{2+}) solution with a molar ratio of 1:1 at pH 5 in the photocatalyst reactor while stirred and irradiated with UV light for 2 h. After photoreaction, the tetrachloroaurate ion ions content was analyzed by AAS, and the photocatalyst material was separated from the solution using an external magnetic bar.

2.3.2. Reduction of $AuCl_4^-$ ions in a mixture with both Cu^{2+} and Ni^{2+} ions

$Fe_3O_4/SiO_2/TiO_2$ nanoparticles photocatalyst weighed 0.025 g was dispersed into the mixture of $AuCl_4^-$, Ni^{2+}, and Cu^{2+} solution with a molar ratio of 1:1:1 in a reactor while being stirred and irradiated with UV light. The solution pH was preset at 5. Irradiation was done for 2 h. After photoreaction, the solid material was separated from the solution using an external magnetic bar, and the metal content was sampled by AAS.

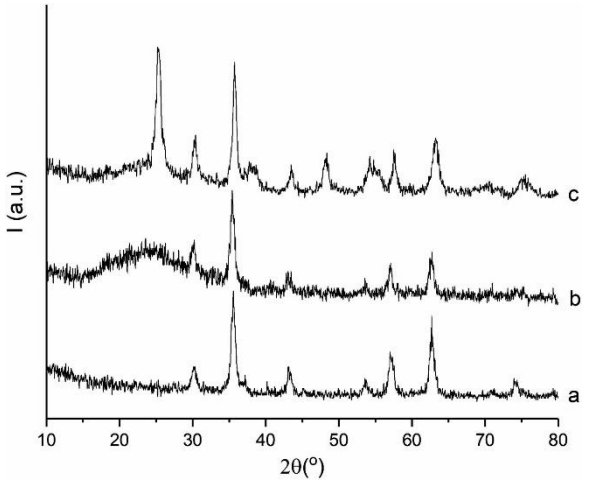

Figure 1. XRD patterns of (a) Fe_3O_4, (b) Fe_3O_4/SiO_2 and (c) $Fe_3O_4/SiO_2/TiO_2$ nanoparticles

3. Results and discussion

3.1. Characterisation of $Fe_3O_4/SiO_2/TiO_2$ nanoparticles

Figure 1 shows the diffraction patterns for Fe_3O_4, Fe_3O_4/SiO_2, and $Fe_3O_4/SiO_2/TiO_2$. The Fe_3O_4 diffractogram agrees with the JCPDS No. 01-1111 as confirmed with the peaks at 2θ = 30.22, 35.56, 43.14, 57.04, and 62.66° (Figure 1a), which indicates face-centered cubic (*fcc*) crystal structure. A similar pattern was observed after coating with SiO_2 with the addition of a wide peak at 2θ about 21-26°. This peak is believed to be due to the amorphous SiO_2 phase. Peaks of the anatase phase of TiO_2 appear at 25.22°, 48.36, and 54.22 on the diffraction pattern of $Fe_3O_4/SiO_2/TiO_2$. A similar result was also reported by previous studies (Kunarti *et al.*, 2016; Kunarti *et al.*, 2017) and literatures (Schatz *et al.*, 2009; Xue *et al.*, 2013).

The TEM images of the obtained nanoparticles are presented in Figure 2. It is observed that there are spherical dark images of Fe_3O_4 core particles covered by a bright shell of SiO_2 and TiO_2 at the outer shell, which very similar brightness with the SiO_2 inner shell. It is believed that TiO_2 coats the outer shell of Fe_3O_4/SiO_2 nanoparticles. The mean diameter of $Fe_3O_4/SiO_2/TiO_2$ nanoparticles is estimated to be 14 nm.

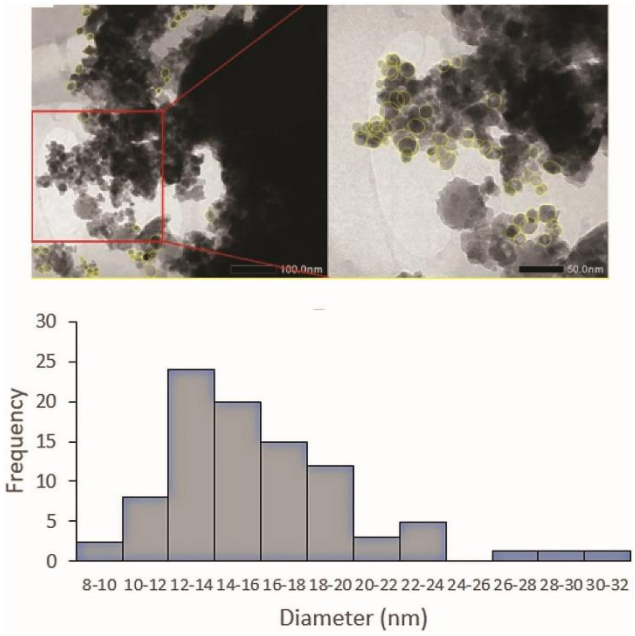

Figure 2. TEM images of Fe_3O_4 nanoparticles after coating with SiO_2 and TiO_2

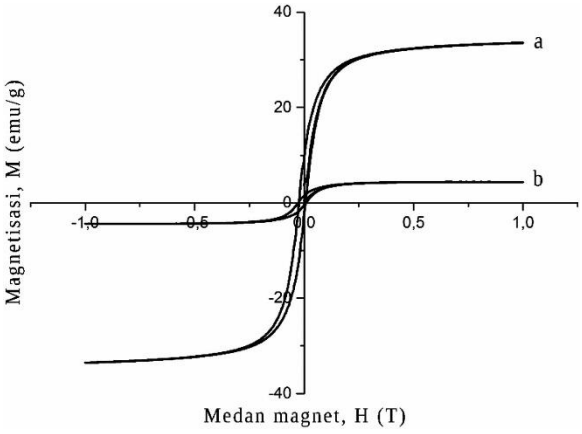

Figure 3. VSM curve of (a) Fe_3O_4, and (b) $Fe_3O_4/SiO_2/TiO_2$ nanoparticles

The magnetic properties of the products were recorded quantitatively by use of a vibrating sample magnetometer (VSM) (Figure 3). The data suggest that there is a decrease in the magnetic properties of Fe_3O_4 after coating with SiO_2 and/or TiO_2. The magnetic hysteresis indicates the superparamagnetic nature of materials. Although there is an appreciable decrease, in general the magnetism of the product is still good (4.38 emu/g). This magnetic property

still allows us to recover the solids by an external magnetic bar after application (Figure 4).

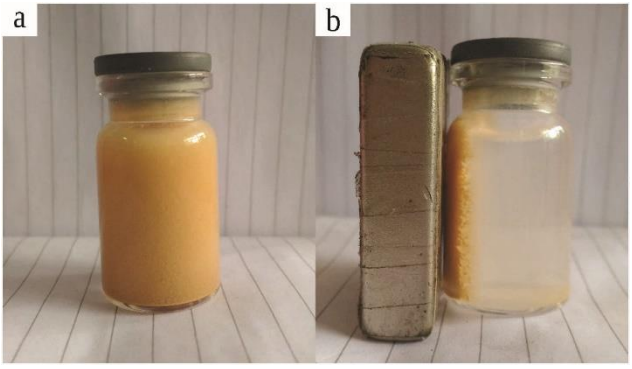

Figure 4. The picture of photocatalyst (a) before and (b) after inteaction with a magnetic bar

3.2. Photocatalytic reduction of tetrachloroauric

3.2.1. The effect of reaction pH

The medium acidity is one of the critical parameters in the photocatalytic reduction process. The pH of the medium affects the charge of the TiO_2 and $AuCl_4^-$ species. Figure 5 shows the effect of pH on $AuCl_4^-$ ion reduction. The photocatalytic reduction increases along with increasing pH and reaches an optimum condition at pH 5. The ease of TiO_2 to give electrons and to form OH is strongly affected by surface speciation of TiO_2. The specification of the surface of TiO_2 (>TiOH) in the aqueous solution is commonly written as follows (Hoffmann *et al.*, 1995)

$$\text{At low pH}: > TiOH + H^+ \rightarrow > TiOH_2^+$$

$$\text{At high pH}: > TiOH + OH^- \rightarrow > TiO^- + H_2O$$

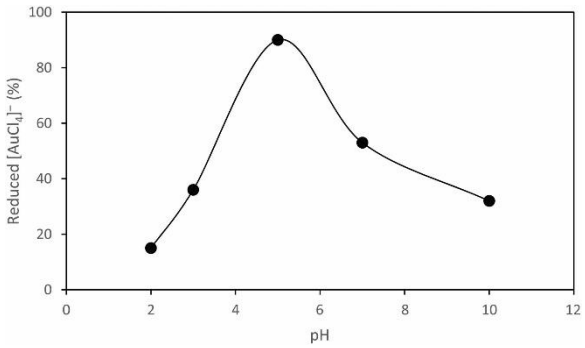

Figure 5. Effect of pH on the photocatalytic reduction of $AuCl_4^-$

At pH less than 3, >TiOH is dominant to form > $TiOH_2^+$. The presence of >TiOH is abundant at pH 3 to 10. Meanwhile, at pH above 10, the >TiOH is dominant as >TiO^-, so at the pH of 5, TiO_2 will be in the form of $TiOH_2^+$ species and the lower the pH, the more $TiOH_2^+$ species. At pH 5, TiO_2 is present as $TiOH_2^+$ species which will interact with anionic charged of $[AuCl_4]^-$ solution. In the presence of UV rays, the photocatalyst will absorb energy from UV rays so that electrons will be transferred from the valence band to the conduction band of $TiOH_2^+$. The $AuCl_4^-$ species will interact with the surface of the photocatalyst, so when $AuCl_4^-$ is on the surface of the photocatalyst, there will be an $AuCl_4^-$ reduction process to metallic gold. At the pH below 5, however, there is a decrease in the reduced $AuCl_4^-$ concentration. This is because the number of $TiOH_2^+$ species is very abundant, resulting in the number of electrons produced decreases. However, when the pH above 5 species of TiO_2 will turn into TiO^- then the interaction between TiO^- and $AuCl_4^-$ becomes difficult result in a lack of $AuCl_4^-$ which can be reduced. In addition, the increase in pH in the solution also causes a species change from $AuCl_4^-$ into precipitation that makes the reduction process ineffective.

3.2.2. The effect of reaction time

Figure 6 shows the effect of the irradiation time on the reduction of $AuCl_4^-$ ions. The longer the irradiation time the more $AuCl_4^-$ to be reduced. A slight decrease in the reduction after 2 h was observed. The number of electrons formed for the occurrence of the reduction process is influenced by the number of rays that affect the photocatalyst surface. Figure 6 shows that at the time of irradiation 0-2 h an increase in $AuCl_4^-$ ion reduction. This is caused by the longtime of irradiation that impacts more photon energy on the photocatalyst. This results in more electrons being formed and the reduction of $AuCl_4^-$ ions to Au^0 will increase. Photoreduction for 2 h is the optimum point of irradiation. In a longer reduction process, the surface of the photocatalyst has been covered by the Au-precipitate resulting from the reduction process thus blocking the interaction between the photocatalyst and the UV light, resulting in constant photocatalytic activity. However, in the results of this study, there is a decrease in the percentage of reduction, this may be due to desorption of the release of $AuCl_4^-$ ions that have bound to $Fe_3O_4/SiO_2/TiO_2$ nanoparticles.

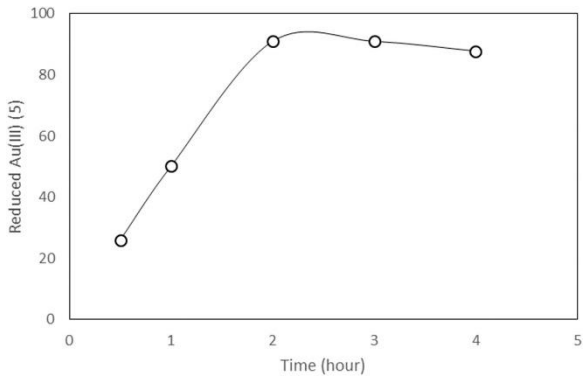

Figure 6. Effect of irradiation time on the photocatalytic reduction of $AuCl_4^-$ to Au^0

3.2.3. The effect of SiO_2 on the catalytic reduction of $AuCl_4^-$

To evaluate the obtained photocatalysts in the reduction of $AuCl_4^-$ ions, the photoreduction reaction was carried out with and without UV light exposure. Figure 7 shows the amount of $AuCl_4^-$ ions both reduced and adsorbed using each of photocatalysts with and without UV light exposure.

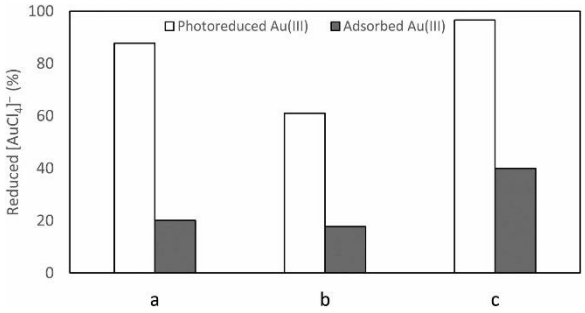

Figure 7. Reduction of $AuCl_4^-$ with photocatalyst of (a) TiO_2, (b) Fe_3O_4/TiO_2 and (c) $Fe_3O_4/SiO_2/TiO_2$

Figure 7 appears that under UV-light irradiation, the $Fe_3O_4/SiO_2/TiO_2$ nanoparticles have a better photocatalytic activity to reduce $AuCl_4^-$ than that of Fe_3O_4/TiO_2, and TiO_2. The Fe_3O_4/TiO_2 nanoparticles have the lowest $AuCl_4^-$ photoreduction activity could be due to direct contact between the TiO_2 and the Fe_3O_4, where the Fe_3O_4 nanoparticles act a recombination center (Beydoun and Amal, 2002). This recombination causes a small number of TiO_2 conduction electrons (e_{cb}-) to play a role in reducing $AuCl_4^-$ ions hence the percentage of $AuCl_4^-$ species is small. This phenomenon did not occur for $Fe_3O_4/SiO_2/TiO_2$, because of the presence of the SiO_2 layer as a charge-transfer insulator was able to prevent electron-hole recombination. This causes the photoreduction activity of $AuCl_4^-$ ions using $Fe_3O_4/SiO_2/TiO_2$ better than that of Fe_3O_4/TiO_2. Meanwhile, the $Fe_3O_4/SiO_2/TiO_2$ nanoparticle has a higher photoreduction activity than TiO_2 due to the presence of the SiO_2 layer (Liu *et al.*, 2011). The SiO_2 layers which have a porous structure can increase the surface area for adsorption so that it facilitates the access of $AuCl_4^-$ Au ions to the photocatalyst active site. In addition, the presence of silica is also capable of immobilizing TiO_2 so that can minimize the agglomeration of TiO_2 particles that may occur in TiO_2 particles. This condition causes the photoreduction process of $AuCl_4^-$ ions using $Fe_3O_4/SiO_2/TiO_2$ to be more efficient.

It is known that the photocatalytic reduction process is initiated and/or accompanied by the adsorption of the species on the TiO_2 surface. Figure 7 shows the results of $AuCl_4^-$ ions adsorption by photocatalysts, in the absence of UV light irradiation. It appears that the $Fe_3O_4/SiO_2/TiO_2$ photocatalyst has the best adsorption ability. The presence of a SiO_2 layer which has a large surface area seems to have better characteristics of mass transfer. The $AuCl_4^-$ adsorption by Fe_3O_4/TiO_2 solid is smaller than that of TiO_2, which is likely due to its lower surface area. It is in good agreement with the previous report (Banisharif *et al*., 2013).

3.2.4. Photocatalytic eduction of $AuCl_4^-$ ions in the presence of Ni^{2+} and Cu^{2+}

Besides gold, nickel and copper are found in electronic waste (Gramatyka *et al.*, 2007). To recover gold from electronic waste, it is first soaked in a strong acid solution to produce $AuCl_4^-$, Ni^{2+}, and Cu^{2+}. Ni^{2+} and Cu^{2+} ions can be photocatalytically reduced by TiO_2 (Joshi *et al.*, 2011). The presence of $Ni^{2+}$and Cu^{2+} ions might affect the photoreduction of $AuCl_4^-$ ions. In this study, $AuCl_4^-$ photoreduction reaction is also carried in the solution containing Ni^{2+} and Cu^{2+} ions. The reaction was performed using $Fe_3O_4/SiO_2/TiO_2$ photocatalyst under UV irradiation. The results are presented in Figure 8.

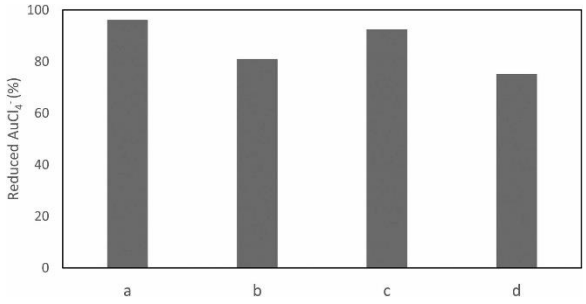

Figure 8. Reduction of $AuCl_4^-$ catalyzed by $Fe_3O_4/SiO_2/TiO_2$ (a) without Ni^{2+} and Cu^{2+}, (b) with Ni^{2+} in the mixture where $AuCl_4^-$ to Ni^{2+} molar ratio 1:1, (c) with Cu^{2+} in the mixture where $AuCl_4^-$ to Cu^{2+} molar ratio of 1:1, and (d) with Ni^{2+} and Cu^{2+} in the mixture where $AuCl_4^-$ to Ni^{2+} to Cu^{2+} molar ratio of 1:1:1

Figure 8 shows that the addition of Ni^{2+} ions causes a decrease in the number of $AuCl_4^-$ ions reduced from 96.13% to 80.98%. In the absence of Ni^{2+} ions, all conduction band (e_{cb}-) electrons produced by TiO_2 are used to reduce Au ions while in the presence of Ni^{2+}ions, both Au ions and Ni^{2+} ions capable of being reduced by TiO_2 so that during the photoreduction reaction takes place, there is competition in the use of the conduction band electrons (e_{cb}-) produced by TiO_2. This causes some conduction band electrons (e_{cb}-) to be used to reduce $AuCl_4^-$ ions and the other part is used to reduce Ni^{2+} ions. Decreasing the number of conduction band electrons (e_{cb}-) to reduce $AuCl_4^-$ ions causes a decrease in reduced $AuCl_4^-$ ions.

Evaluation of $Fe_3O_4/SiO_2/TiO_2$ activity for $AuCl_4^-$ ion reduction was also made by comparing the photocatalytic activity of $Fe_3O_4/SiO_2/TiO_2$ in the presence of Cu^{2+} ions with the molar ratio of 1:1 under UV illumination. The result is presented in Figure 8. It shows a slight decrease in the percentage reduction of Au ions in the mixture of $AuCl_4^-$ and Cu^{2+} ions. It can be concluded that the presence of Cu^{2+} ions can decrease the percentage reduction of $AuCl_4^-$ ions although relatively small and insignificant. This is because the Cu^{2+} ions in the solution can also be reduced to cause competition with $AuCl_4^-$ ions in binding the electrons. However, since the reduction of Cu^{2+}ions is slower, which is indicated by a value of E^0 (E^0 = 0.340 eV) which is much lower than that of $AuCl_4^-$ ions (E^0 = 1.002 eV). The Cu^{2+} ions are more difficult to be reduced than $AuCl_4^-$ ions so that the presence of Cu^{2+} ions does not significantly affect the $AuCl_4^-$ ion reduction.

Reduction of $AuCl_4^-$ was also performed in the presence of Ni^{2+} and Cu^{2+}. Figure 8 reveals that the presence of Ni^{2+} and Cu^{2+} leads to a decrease in $AuCl_4^-$ photoreduction. The addition of Ni^{2+} has a stronger effect than that of Cu^{2+}. Both Ni^{2+} and Cu^{2+} can be reduced, as suggested by their standard reduction potentials of -0.25 V and 0.34 V, to form Ni^0 and Cu^0 respectively, which competes with $AuCl_4^-$ photoreduction. The standard reduction potentials of Ni^{2+}

and Cu^{2+} are much lower than those of $AuCl_4^-$, which is much more difficult to reduce than $AuCl_4^-$. Based on their standard reduction potential, Cu^{2+} is easier to reduce than Ni^{2+}. However, the opposite result is observed. $AuCl_4^-$ ions are reduced directly to Au^0 ions while Cu^{2+} ions may be reduced to Cu^+ and Cu^0. When Cu^+ and Cu^0 species escape from the surface of TiO_2 and meet with $AuCl_4^-$ ions, there will be redox reaction among $AuCl_4^-$, Cu^+ and Cu^0 ions where Cu^+ and Cu^0 will oxidize back to Cu^{2+} ions. The $AuCl_4^-$ has a higher reduction potential value so it is reduced, while Cu^+ and Cu^0 which have a smaller reduction potential value then they are oxidized. The cross-redox reaction interface probably happens, in which the $AuCl_4^-$ reduction can occur because of the bridge of the previously reduced Cu^{2+} ions. So that the only small decreased of $AuCl_4^-$ ion reduction process in the presence of Cu^{2+} ion in this study is probably affected by the reduction potential values of each metal ions as well as the crossing redox reaction interface effect. Meanwhile, this phenomenon does not happen for Ni^{2+} ion. Moreover, the decrease in the amount of reduced $AuCl_4^-$ ions in the mixture of $AuCl_4^-$, Ni^{2+}, and Cu^{2+} in Figure 8 more likely due to the deposition of nickel and copper on the surface of the photocatalyst, so active site of the photocatalyst is covered by metal thereby reducing the amount of reduced $AuCl_4^-$. The presence of Ni^{2+} and Cu^{2+} ions in the mixture slightly hinder the reduction of $AuCl_4^-$.

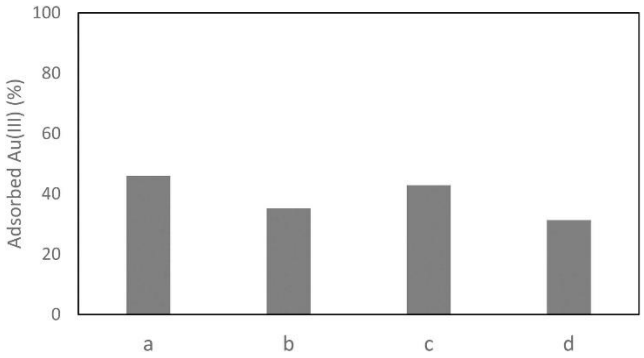

Figure 9. Adsorption of $AuCl_4^-$ by $Fe_3O_4/SiO_2/TiO_2$ (a) without Ni^{2+} and Cu^{2+}, (b) with Ni^{2+} in the mixture where $AuCl_4^-$ to Ni^{2+} molar ratio of 1:1, (c) with Cu^{2+} in the mixture where $AuCl_4^-$ to Cu^{2+} molar ratio of 1:1, and (d) with Ni^{2+} and Cu^{2+} in the mixture where $AuCl_4^-$ to Ni^{2+} to Cu^{2+} molar ratio of 1:1:1

The stronger effect is shown by the presence of Ni^{2+}. It is clearly not caused by competition in the photoreduction, but it prominently caused by adsorption of Ni^{2+} on the surface of TiO_2. As presented previously, the photocatalytic reduction process is always initiated and/or accompanied by adsorption on the surface of photocatalyst (Wahyuni *et al.*, 2015; Kunarti *et al*., 2017). When $AuCl_4^-$ in the solution is along with Ni^{2+} and Cu^{2+} ions, the adsorption of the three ions should be involved. The Ni^{2+} and Cu^{2+} ions having a smaller size than $AuCl_4^-$, can be adsorbed faster than Au(III). Consequently, the adsorption of $AuCl_4^-$ is inhibited by Ni^{2+} and Cu^{2+}, causing a decrease in the $AuCl_4^-$ adsorption, and so the lower photoreduction. This result is in accordance with the previous study in the reduction of $AuCl_4^-$ using TiO_2 as the photocatalyst (Wahyuni *et al.*, 2015). The role of Ni^{2+} and Cu^{2+} in the lowering $AuCl_4^-$ photoreduction caused by adsorption competition is supported by data obtained from a process without light exposure as illustrated by Figure 9. It is seen in the figure that adsorption of $AuCl_4^-$ decreased in the presence of Ni^{2+} but only slightly decreased when Cu^{2+} is present.

As discussed earlier, at pH 5 the surface of TiO_2 is dominated by $TiOH_2^+$ and TiOH groups, hence the species $AuCl_4^-$ and $AuCl_3OH^-$ ions are adsorbed through the complex formation and electrostatic interactions. It has also been reported that at pH 5 or lower, Ni^{2+} and Cu^{2+} ions are dominant. This makes an electrostatic interaction between the Ni^{2+} ion and the positively charged surface of $TiOH_2^+$ is not possible to occur so that the adsorption of Ni^{2+} ions on the photocatalyst surface is likely to occur through electrostatic interactions between Ni^{2+} ions and SiO_2. This phenomenon also takes place for Cu^{2+} ions.

SiO_2 has a pH_{pzc} (potential zero charges) value of about 2.0, therefore at pH 5, the SiO_2 has a negatively charged surface. The porous structure of TiO_2 allows a silica layer to have contact with the solution. So that electrostatic interactions between SiO_2 and Ni^{2+} and Cu^{2+} can occur. In addition, the adsorption process of Ni^{2+} and Cu^{2+} ions can also take place through the interaction between these ions and free electron pairs on oxygen atoms on the surface of >TiOH. The interaction between TiO_2 and Ag^+ ions has also been reported previously (Kunarti *et al*., 2017). Adsorbed Ni^{2+} and Cu^{2+} can cover the surface of $Fe_3O_4/SiO_2/TiO_2$ nanoparticles to prevent adsorption of either $AuCl_4^-$ or $AuCl_3OH^-$ and prevent further reduction. Therefore, the presence of Ni^{2+} and Cu^{2+} ions slow down the photoreduction of $AuCl_4^-$ as indicated in Figure 9(d).

4. Conclusions

The $AuCl_4^-$ ions have been photocatalytically reduced to metallic gold using $Fe_3O_4/SiO_2/TiO_2$ nanoparticles as photocatalyst. The $Fe_3O_4/SiO_2/TiO_2$ nanoparticles were prepared by combined methods of co-precipitation, sonochemical and sol-gel synthesis, as well as calcination at 500 °C. The products have magnetic moment of 4.38 emu/g, which could be separated from the solution mixture by using an external magnetic bar. The materials photocatalytically reduced 96 % of $AuCl_4^-$ ions in the solution, at 0.025 g photocatalyst loading, 50 mg L^{-1} $AuCl_4^-$ solution concentration under UV light illumination. The addition of Ni^{2+} and Cu^{2+} ions decreases the amount of the ions to be reduced due to the competition between reduction and adsorption processes. This prepared photocatalyst is expected to find application in the recovery of gold from electronic waste, which are abundant and complex.

Acknowledgements

The authors acknowledge to Universitas Gadjah Mada and Faculty of Mathematics and Natural Sciences for the financial support.

References

Álvarez P.M., Jaramillo J., López-Piñero F. and Plucinski P.K. (2010), Preparation and characterization of magnetic TiO_2

nanoparticles and utilization for the degradation of emerging pollutants in water, *Applied Catalalysis B: Environmental*, **100**, 338–345.

Banisharif A., Elahi S.H., Firooz A.A., Khodadadi A.A. and Mortazavi Y. (2013), TiO_2/Fe_3O_4 nanocompositep Photocatalysts for enhanced photo-decolorization of congo red dye, *International Journal of Nanoscience and Nanotechnology*, **9**, 193–202.

Barakat M.A. (2010), New trends in removing heavy metals from industrial wastewater, *Arabian Journal of Chemistry*, **4**, 361–377.

Beydoun D. and Amal R. (2002), Implications of heat treatment on the properties of a magnetic iron oxide-titanium dioxide photocatalyst, *Materials Science and Engineering*, **94**, 71–81.

Beydoun D., Amal R., Low G.K.-C. and McEvoy S. (2000), Novel photocatalyst: titania-coated magnetite activity and photodissolution, *Journal of Physical Chemistry B*, **104**, 4387–4396.

Cui J. and Zhang L. (2008), Metallurgical recovery of metals from electronic waste: a review, *Journal of Hazardous Materials*, **158**, 228–256.

Fajri M.L. (2017), Synthesis of $Fe_3O_4/SiO_2/TiO_2$ nanocomposites as photocatalyst for reduction of Au(III) ion in the mixture of Au(III) and Ni(II) ions, Undergraduate Thesis, Deptartement of Chemistry, Universitas Gadjah Mada.

Gad-Allah T.A., Kato S., Satokawa S. and Kojima T. (2007), Role of core diameter and silica content in photocatalytic activity of $TiO_2/SiO_2/Fe_3O_4$ composite, *Solid State Science*, **9**, 737–743.

Gramatyka P., Nowosielski R. and Sakiewicz P. (2007), Recycling of waste electrical and electronic equipment, *Journal of Achievements in Materials and Manufacturing Engineering*, **20**, 535–538.

Grieken R.V., Aguado J., Maria-José M.L. and Marugán J. (2005), Photocatalytic gold recovery from spent cyanide plating bath solution, *Gold Bulletin*, **38**, 180–187.

Hoffmann M.R., Martin S.T., Choi W. and Bahnemann D.W. (1995), Environmental applications of semiconductor photocatalysis, *Chemical Reviews*, **95**, 69–96.

Joshi K.M., Patil B.N., Shirsath D.S. and Shrivastava V.S. (2011), Photocatalytic removal of Ni(II) and Cu(II) by Using different semiconducting materials, *Advances in Applied Science Research*, **2**, 445–454.

Kida T., Oshima R., Nonaka K., Shimanoe K. and Nagano M. (2009), Photoinduced recovery of gold using an inorganic/organic hybrid photocatalyst, *Journal of Physical Chemistry C*, **113**, 19986–19993.

Kunarti E.S., Roto R., Pradipta A.R. and Budi I.S. (2017), $Fe_3O_4/SiO_2/TiO_2$ nanoparticles as catalyst for Ag(I) ions, *Oriental Journal of Chemistry*, **33**(4), 1933–1940.

Kunarti E.S., Syoufian A., Budi I.S. and Pradipta A.R. (2016), Preparation and properties of $Fe_3O_4/SiO_2/TiO_2$ core/shell nanocomposite as recoverable photocatalyst, *Asian Journal of Chemistry*, **28**, 1343–1346.

Liu H., Jia Z., Ji S., Zheng Y., Li M. and Yang H. (2011), Synthesis of $TiO_2/SiO_2@Fe_3O_4$ magnetic microspheres and their properties of photocatalytic degradation dyestuff, *Catalysis Today*, **175**, 293–298.

Rottman J., Platt L.C., Sierra-Alvarez R. and Shadman F. (2013), Removal of TiO_2 nanoparticles by porous media: effect of filtration media and water chemistry, *Chemical Engineering Journal*, **217**, 212–220.

Schatz A., Hager M. and Reiser O. (2009), Cu(II)-azabis (oxazoline)-complexes immobilized on superparamagnetic magnetite/silica nanoparticles: a highly selective and recyclable catalyst for the kinetic resolution of 1,2-diols, *Advanced Functional Materials*, **19**, 2109–2115.

Szabo T., Veres A., Cho E., Khim J., Varga N. and Dekany I. (2013), Photocatalyst separation from aqueous dispersion using graphene oxide/TiO_2 nanocomposites, *Colloids and Surfaces A: Physicochemical and Engineering Aspects*, **433**, 230–239.

Ullah S., Ferreira-Neto E.P., Pasa A.A., Alcântara C.C.J., Acuña J.J.S., Bilmes S.A., Ricci M.L.M., Landers R., Fermino T.Z. and Rodrigues-Filho U.P. (2015), Enhanced photocatalytic properties of core@shell $SiO_2@TiO_2$ nanoparticles, *Applied Catalysis B: Environmental*, **179**, 333–343.

Wahyuni E.T., Kuncaka A. and Sutarno S. (2015), Application of photocatalytic reduction method with TiO_2 for gold recovery, *American Journal of Analytical Chemistry*, **3**, 207–211.

Wojnicki M., Tokarski T. and Kwolek P. (2013), Kinetic study of the photoelectrochemical gold recovery from diluted chloride solutions, *Archives of Metallurgy and Materials*, **58**, 709–716.

Xi W. and Geissen S.U. (2001), Separation of titanium dioxide from photocatalytically treated water by cross-flow microfiltration, *Water Reserch*, **35**, 1256–1262.

Xue C., Zhang Q., Li J., Chou X., Zhang W., Ye H., Cui Z. and Dobson P.J. (2013), High photocatalytic activity of Fe_3O_4-SiO_2-TiO_2 functional particles with structure, *Journal of Nanomaterials*, 2013, 1–8.